THE JOURNAL OF
PHYSICAL CHEMISTRY A

Competition between a Tetrel and Halogen Bond to a Common Lewis Acid

Published as part of The Journal of Physical Chemistry virtual special issue "Alexander Boldyrev Festschrift".

Steve Scheiner*

Cite This: *J. Phys. Chem. A* 2021, 125, 308−316 Read Online

ABSTRACT: The T and X atoms of TF_3X (T = C, Si, Ge, Sn; X = Cl, Br, I) can engage in a tetrel or halogen bond, respectively, with an approaching NH_3 base. With the exception of T = C, the tetrel bonds are considerably stronger than the halogen bond regardless of the nature of T or X. Because both bonds involve electron acceptance by the central TF_3X Lewis acid, there is a negative cooperativity between these two bonds when both are present. The halogen bond is weakened much more than is the tetrel bond and is in fact completely disrupted in some cases. Replacement of the three F substituents on TF_3X by H attenuates the σ-holes on both T and X atoms, weakens and stretches both bonds, and eliminates any halogen bonds involving Cl. Even in those cases where a halogen bond does occur in the dimer, this bond cannot withstand the presence of a simultaneous tetrel bond and so disappears.

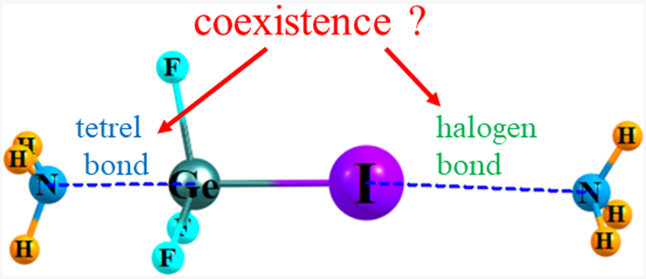

■ INTRODUCTION

Among the pantheon of noncovalent bonds, the H-bond has undergone the longest and most intense scrutiny over the years, which has led to a thorough understanding of the sources of its stability.[1−6] Recent years have focused attention on a number of close parallels of the H-bond where the bridging proton is replaced by one of numerous other atoms.[7−20] Of these, the halogen bond (XB) is the most well-known and has the longest history. Despite the high electronegativity of the halogen atom, and its consequent overall partial negative charge, it is nevertheless able to develop a small positive region directly along the extension of the R−X covalent bond, where X refers to any halogen atom and R to its substituent. This positive area is commonly termed a σ-hole and attracts a nucleophile in the same manner as does the proton in a H-bond. Also like the H-bond, the XB is the beneficiary of other attractive forces, such as charge transfer and dispersion.

It is not only the halogen family that can act in this manner but also other electronegative atoms on the right side of the periodic table.[21] These bonds are typically dubbed chalcogen and pnicogen bonds, in accord with the family of elements from which it is drawn. Perhaps the least studied of this category is the tetrel bond (TB),[22−35] whose bridging atom comes from the like-named family composed of C, Si, Ge, and so on. As research has continued on these sorts of noncovalent bonds, their importance to a wide array of chemical and biological processes is becoming increasingly recognized.[36−47]

Just like H-bonds, these sister interactions are also subject to cooperativity effects.[29,48−55] It is understood that the whole can be greater or less than the sum of its parts. In particular, if the central molecule B in a A··B··C triad serves as both electron donor and acceptor, the overall binding energy of this triad will be greater than the sum of the A··B and B··C binding energies in the individual dyads, i.e., positive cooperativity. The opposite effect of a weakening force or negative cooperativity will be the product if B must serve as double donor or double acceptor. The question thus arises as to whether the latter negative cooperativity would be sufficient to cause one of these two noncovalent bonds to break. That is, if a third molecule C is added to a A··B dimer, such that B would be a double electron acceptor in a putative A··B··C trimer, would this addition cause the breakage of the A··B bond, leaving only B··C? Or to pose the question in an alternate manner, might the pre-existing A··B dimer prevent the C unit from binding to B at all?

It is the goal of the current investigation to probe this question in some detail. The two types of bonds that are the focus of this work are the halogen and tetrel bond. A host of prior calculations

Received: November 7, 2020
Revised: December 8, 2020
Published: December 22, 2020

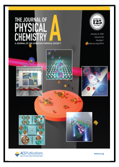

https://dx.doi.org/10.1021/acs.jpca.0c10060

have shown that these two bonds tend to be of comparable strength and obey similar patterns related to atom size, electronegativity, polarizability, and substituent effects. So the question as to which bond might dominate the other is an open question. Can both of these bonds coexist to a central molecule acting as electron acceptor to both? Or might a tetrel-bonded dimer be pulled apart if a halogen bond is formed to one of its constituents, or vice versa? The present work applies quantum calculations to this question, using a wide variety of different molecules to provide as general an answer as possible.

SYSTEMS AND METHODS

A tetrel (T) and a halogen (X) atom were placed in competition with one another in the context of a T−X bond which a nucleophile could approach from either end. Calculations thus focused on the TF_3X set of molecules where T ran the gamut from C to Si, Ge, and Sn, while X was chosen from the set of Cl, Br, and I. The three electron-withdrawing F substituents on this molecule were chosen so as to maximize any σ-hole that might appear on the T and X atoms. These F centers were next replaced by H so as to examine the consequence of weakening these σ-holes upon the competition between the T and X atoms for a nucleophile. The consideration of both TF_3X and TH_3X ought to thus cover a full range of nucleophilicity. NH_3 was chosen as the universal base first for its medium strength as a nucleophile whose N lone pair can be donated to a Lewis acid. Its small size minimizes secondary interactions that might otherwise complicate the analysis. An added bonus is the numerous other works in the literature in which NH_3 has been used as prototype base with which the data computed here may be directly compared. The diverse set of systems considered here are displayed in Scheme 1.

Scheme 1

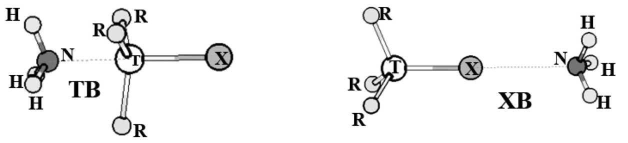

T=C,Si,Ge,Sn
X=Cl,Br,I
R=F,H

The M06-2X DFT functional was used in concert with the aug-cc-pVDZ basis set within the framework of the Gaussian-09[56] set of programs. This level of theory has been applied to good account in numerous previous studies[57−65] of related systems. To account for relativistic effects, the aug-cc-pVDZ-PP pseudopotential[66,67] was applied to Sn and I. All geometries were fully optimized with no symmetry restrictions. The interaction energy, E_{int}, was evaluated as the difference between the energy of the complex and the sum of the energies of monomers in the geometries they adopt within the complex. The counterpoise[68−70] procedure was used to correct basis set superposition error. Molecular electrostatic potentials (MEPs) and their extrema were evaluated with the Multiwfn program.[71] The AIMALL program[72] was used to analyze the electron density and in particular the bond paths and the characteristics of their critical points. Charge transfers between orbitals and their energetic consequences were considered in the context of the natural bond orbital (NBO) prescription.[73,74]

RESULTS

TF_3X. *Geometries and Energetics.* The ability of the various TF_3X molecules to engage in either a TB or XB complex with a base like NH_3 will be based in part on the depth of the σ-hole that exists on the T or X atoms, respectively. The maxima of the MEP in these two positions are displayed in Table 1 to lie in the general range of 15−63 kcal/mol so ought to be sufficient for this purpose. (The T maximum displayed is that lying opposite the X atom.) There are a number of regular patterns in these quantities that will impact the competition between these two σ-holes to attract a base. First with respect to those on the T atoms, V_{max} grows along with the size of the T atom. For a given T, the diminishing electronegativity of the Cl > Br > I atoms leads to a like weakening of the σ-hole in the same order. Consequently, the largest V_{max} of 62.7 kcal/mol is associated with the SnF_3Cl monomer. This same diminishing electronegativity has the opposite effect of a growing V_{max} on the X atom. The sensitivity of the X σ-hole to the T atom is not as regular, although there is a general increasing trend for larger T, such that the most intense X σ-hole of 35.6 kcal/mol occurs on the I atom of SnF_3I. The σ-hole on the T atom is uniformly stronger than that on X, hence the positive values in the last column of Table 1, with the single exception of CF_3I. This exception is a result of a conflation of trends with larger X, the dropping T V_{max} coupled with the rise in the X σ-hole. To this is added the fact that the V_{max} on T is especially small for T = C.

Table 1. Maximum of Molecular Electrostatic Potential V_{max} (kcal/mol) on ρ = 0.001 Au Isodensity Surface of TF_3X at Indicated Atom and the Difference between T and X Maxima

T	X	T[a]	X	T−X[b]
C	Cl	21.13	20.29	0.84
	Br	23.10	21.03	2.07
	I	18.48	31.63	−13.15
Si	Cl	41.32	14.59	26.73
	Br	39.58	19.40	20.18
	I	36.65	27.85	8.80
Ge	Cl	47.11	18.15	28.96
	Br	43.56	24.21	19.35
	I	38.09	34.62	3.47
Sn	Cl	62.71	16.99	45.72
	Br	58.46	23.96	34.50
	I	50.43	35.57	14.86

[a] Maximum opposite X atom. [b] Difference between T and X quantities.

Examples of systems in which TF_3X engage in a tetrel or halogen bond with NH_3 are provided in Figures 1a and 1b, respectively, for GeF_3I. All dimers are within 2°−3° of a strict XT··N or TX··N linearity, respectively. A simultaneous interaction of both sorts with a pair of NH_3 units is illustrated in Figure 1c. NH_3 can engage in a TB with all of the various TF_3X molecules, with intermolecular $R(T\cdot\cdot N)$ distances listed on the left side of Table 2. These TB distances are fairly insensitive to the X atom, despite the sensitivity of the T σ-hole to X. $R(T\cdot\cdot N)$ grows along with the size of the T atom, with the exception of CF_3X which has considerably longer separations.

The $R(X\cdot\cdot N)$ distances on the right side of Table 2 are considerably longer than $R(T\cdot\cdot N)$, suggesting weaker bonds. Moreover, the $R(X\cdot\cdot N) - R(T\cdot\cdot N)$ difference is quite substantial, on the order of a full angstrom for most complexes. The exceptions are CF_3Cl and CF_3I, where the halogen bond is shorter than the TB, and the T and X σ-holes are of comparable

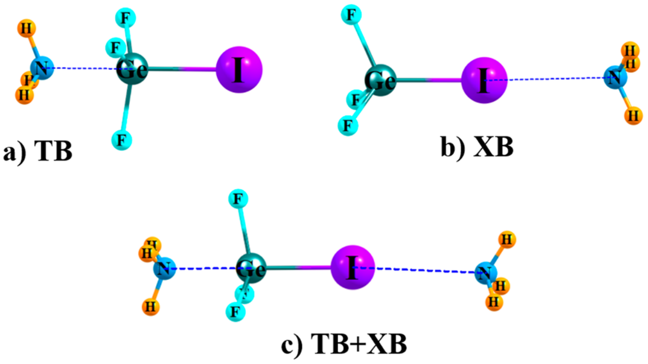

Figure 1. Geometries of (a) TB, (b) XB, and (c) TB + XB complexes of GeF_3I with one or two molecules of NH_3.

depth. Another interesting feature of the halogen bond lengths is their insensitivity to both X and T, being roughly equal to 3.1–3.2 Å for most systems. This insensitivity is surprising in light of the strong variations in the X V_{max} in Table 1. This small variation is likely due to a compensation between larger X atoms on one hand and deeper σ-holes on the other.

The interaction energies in Table 3 show that, with the exception of T = C, the TBs are far more stable than are the XBs. The TB interaction energies are in the 35–37 kcal/mol range, far exceeding those for the XBs that do not exceed 6 kcal/mol. It is also interesting to note the very narrow range of TB energies, which have little dependence upon the nature of T or X, or the value of V_{max}. This small range is in keeping with the lack of variability of the R(T··N) TB bond lengths. Unlike the TBs, the XB interaction energies are sensitive to the identity of the X atom, with a milder dependence upon T. With respect to the T = C systems, it is the halogen bond that is the stronger of the two. This reversal is primarily due to the very weak TBs, barely more than 1 kcal/mol. These weaker TBs are consistent with the lesser V_{max} for the C atom, but E_{int} is disproportionately reduced as compared to the σ-hole intensity.

Wave Function Analysis. The next two columns of Table 3 provide a measure of bond strength arising from AIM analysis of the wave functions. The bond critical point densities mimic the behavior of the interaction energies. ρ_{BCP} is very much larger for TB as compared to XB. This quantity is roughly constant for all the TBs, whereas it grows along with the size of X for the XBs. The numerical values of the TBs are roughly equal to 0.07 au, consistent with a strong noncovalent bond, while the XB quantities of only about 0.01 are what one might expect for interaction energies <5 kcal/mol. Again, the behavior of the C-systems is quite different. In fact, AIM analysis indicates these are not tetrel bonds at all, as the bond paths from the N of NH_3 lead instead to the three F atoms of CF_3X, so might better fit the description of a trifurcated N··F bond.

NBO treatment provides a picture of charge transfer from one orbital to another. In particular, the parameters listed in the last three columns of Table 3 refer to transfer from the N lone pair of NH_3. In the case of the halogen-bonded complexes, the charge is transferred primarily into the σ^*(TX) antibonding orbital which is collinear with the X σ-hole. The TB utilizes two destinations. It can first transfer into the σ^*(TX) antibonding orbital lying directly opposite the N but also those involving the three TF bonds. Indeed, Table 3 indicates the sum of the latter three transfers exceeds that of the former. The patterns of the $E(2)$ data are again consistent with the energetics. The TB transfer energetics dwarf those for the XBs. There is only mild sensitivity of the TB parameters to T or X, whereas $E(2)$ increases with X size for the halogen bonds. It might be noted parenthetically that the R(Si··N) bonds are short enough that NBO fails to view the complex as two separate entities and that the C system TBs are far weaker than are the others.

Another consequence of each noncovalent bond is its effect upon the internal T–X covalent bond. The changes imposed on both the length of this bond and its vibrational stretching frequency are displayed in Table 4. The formation of the tetrel bond causes a substantial elongation of the bond, as much as 0.1 Å in some cases. This stretch is maximized for T = Si, followed by Ge and then Sn, and grows along with halogen size: Cl < Br < I. Formation of the halogen bonds produces an opposite effect of a small bond contraction, with the exceptions occurring for X = I for which the T–I bond elongates.

With respect to the vibrational frequencies in the right half of Table 4, it must first be understood that the T–X stretching mode becomes coupled to varying degrees with the ν(T–N) stretch due to the strength of the TB, and the amount of this coupling is associated with both bond strengths and atomic masses. This coupling causes certain deviations from a simple relationship between $\Delta\nu$ and TB bond strength. Nonetheless, there is a fairly large red-shift for the TB systems in most cases,

Table 2. Intermolecular N··T/X Distances (Å) between NH_3 and T or X Atoms of TF_3X and Deviations from Strict Linearity in Trimers

		TB			XB			
T	X	dimer	trimer	trimer−dimer	dimer	trimer	trimer−dimer	$\Delta\theta$,[a] deg
C	Cl	3.221	3.269	0.048	2.983	3.041	0.058	21.0[b]
	Br	3.238	3.328	0.090	3.018	3.037	0.019	9.5[b]
	I	3.226	3.313	0.087	2.979	3.011	0.032	14.3[b]
Si	Cl	2.043	X		3.187	X		
	Br	2.040	2.056	0.016	3.191	3.508	0.317	14.1
	I	2.042	X		3.229	X		
Ge	Cl	2.124	X		3.138	X		
	Br	2.124	2.134	0.010	3.120	3.344	0.224	36.4
	I	2.129	2.149	0.020	3.104	3.307	0.203	8.6
Sn	Cl	2.281	2.281	0.000	3.108	3.457	0.349	13.9
	Br	2.284	2.288	0.004	3.106	3.262	0.156	12.1
	I	2.284	2.291	0.007	3.093	3.260	0.167	0.3

[a] Angle between X··N axis and trisector of the NH_3 unit. [b] Angle between C··N axis and trisector of the NH_3 unit.

Table 3. Interaction Energies, Bond Critical Point Densities, and NBO Values of $E(2)$ for Transfer from the NH_3 N Lone Pair in $(NH_3)_nTF_3X$

			$-E_{int}$, kcal/mol		ρ_{BCP}, 10^{-4} au		$E(2)$, kcal/mol		
T	X	n	TB	XB	TB[a]	XB	TB		XB
							σ^*(TX)	$\Sigma\sigma^*$(TF)	σ^*(TX)
C	Cl	1	1.35	2.74	3Fx80	131	0.40	0.32	2.59
		2			3Fx72	118	0.31	0.23	2.13
	Br	1	1.39	4.06	3F x36	145	0.37	0.34	4.43
		2			3Fx79	140	0.36	0.34	4.10
	I	1	1.15	6.61	3Fx78	190	0.29	0.46	9.48
		2			3Fx70	180	0.21	0.32	8.52
Si	Cl	1	35.99	1.67	633	94	[b]		0.86
	Br	1	36.70	2.64	637	110	[b]		1.68
		2			618	63	[b]		0.48
	I	1	36.92	4.23	633	126	[b]		3.16
		2			623	80	23.82	73.40	0.90
Ge	Cl	1	35.59	2.18	711	102	19.58	72.31	1.12
	Br	1	35.57	3.48	711	125	20.01	73.92	2.24
		2			696	80	18.91	73.22	0.66
	I	1	34.85	5.62	703	157	20.22	75.52	4.87
		2			672	110	18.31	72.80	2.25
Sn	Cl	1	37.75	2.08	619	109	11.72	63.11	1.38
		2			619	57	11.05	63.58	0.32
	Br	1	37.14	3.58	615	129	11.86	64.30	2.51
		2			610	98	10.93	64.58	1.15
	I	1	36.33	5.95	614	162	11.80	66.54	4.96
		2			605	120	10.73	66.68	2.36

[a] T··N unless F··N as indicated by F designation. [b] NBO method considers the whole complex as a single unit.

Table 4. Change in T−X Bond Length and Vibrational Stretching Frequency Caused by Complexation

		r(T−X), Å			ν(T−X), cm^{-1}		
		dimer		trimer	dimer		trimer
T	X	TB	XB		TB	XB	
C	Cl	0.0128	−0.0046	0.0049	−20.9	10.0	−6.8
	Br	0.0148	−0.0019	0.0098	−23.6	13.4	−3.4
	I	0.0104	0.0025	0.0095	−21.4	19.8	3.1
Si	Cl	0.0739	−0.0051	X	−15.9	3.0	X
	Br	0.0878	−0.0021	0.0791	3.7	1.5	2.6
	I	0.0964	0.0019	X	7.8	−0.8	X
Ge	Cl	0.0561	−0.0041	X	−45.6	4.9	X
	Br	0.0625	−0.0009	0.0560	−18.9	1.8	−14.2
	I	0.0691	0.0081	0.0638	−0.8	1.5	−5.9
Sn	Cl	0.0314	−0.0043	0.0237	−11.1	1.3	−5.8
	Br	0.0366	−0.0003	0.0291	−12.5	−0.1	−4.6
	I	0.0394	0.0093	0.0360	13.3	−0.9	21.1

with some exceptions. Frequency displacements caused by the XB are smaller and usually to the blue. The larger shifts associated with the C−X halogen bonds can be connected with both the fairly strong XBs and the lighter mass of C. It should be stressed finally that most of the T−X stretches of the TBs are reflected in frequency shifts to the red, while blue-shifts are associated with the TX bond contractions in the XBs.

Trimers. An important question addresses the competition between the two potential types of bond, TB vs XB. Because both sorts of bonding involve charge transfer to the TF_3X molecule from the approaching base, one would expect the presence of one bond ought to inhibit formation of the other. Judging by the much stronger TBs as compared to XBs in Table 3, it would be logical to presume that if any bond were to be displaced by the other, it ought to be the latter. And in fact the X demarcations in Table 2 show that when confronted by a valid TB, the SiF_3Cl, SiF_3I, and GeF_3Cl units are incapable of engaging in a XB as well. Even in some of those cases where the $TF_3X + (NH_3)_2$ trimer represents a stable minimum, there are some geometric deviations from a strictly linear arrangement, involving a rotation of the NH_3 lone pair away from the X atom by a certain amount. These deviations from strict linearity are reported in the last column of Table 2 and reflect the weakness of any halogen bond in these trimers.

Table 3 shows the way in which formation of the third bond affects the AIM and NBO properties of the other. Taking the GeF_3I unit as an example, the formation of the XB causes the TB ρ_{BCP} of $H_3N\cdots GeF_3I$ system to drop from 0.0703 to 0.0672 au. Likewise, the halogen bond in $GeF_3I\cdots NH_3$ is reduced from 0.0157 to 0.0110 au when the TB is formed with another NH_3 unit. Both of these reductions conform to the idea of negative cooperativity. The general pattern observed in Table 3 is that the formation of the XB has much less of a reducing effect on the TB than vice versa. The NBO data in the last columns of Table 3 agree with this same pattern that the formation of the second bond weakens the first and that it is the XB that suffers the greatest diminution.

The changes undergone by the internal TX bond are displayed in the trimer columns of Table 4 for the full trimer, containing both a TB and XB. These changes take on the same sign as that observed in the TB dimer, consistent with the greater strength and perturbing effect of the latter as compared to the XB. But because the individual TB and XB generally have opposite effects, the magnitudes of both Δr(TX) and $\Delta\nu$(TX) take on the sign in the TB system, albeit of lesser magnitude.

TH_3X. *Geometries and Energetics.* The presence of the three electron-withdrawing F atoms on the TF_3X molecule might perhaps be responsible for a distortion of the relative abilities of the T and X atoms to engage in noncovalent bonding with an approaching base. So additional calculations were performed with all three F atoms replaced by H. This substitution retains the σ-holes as before but clearly diminishes their depth, as described in Table 5. But importantly, it is the magnitude of V_{max} on the X atom that suffers a considerably larger drop as compared to T. The σ-hole on T is reduced by some 2−12 kcal/mol while that on X drops by 17−31 kcal/mol. The electrostatic picture thus offers a large advantage to complexation with T over X, as indicated by the last column of Table 5. Indeed, the values of V_{max} for the X atom are small enough, and in some cases of negative sign, so there is some question as to whether a halogen bond can form at all.

Table 5. Maximum of Molecular Electrostatic Potential V_{max} (kcal/mol) on ρ = 0.001 Au Isodensity Surface of TH_3X at Indicated Atom

		T	X	T−X
C	Cl	17.40	−0.46	17.86
	Br	16.87	4.24	12.63
	I	13.12	13.88	−0.76
Si	Cl	35.16	−2.98	38.14
	Br	34.78	1.85	32.93
	I	32.69	9.67	23.02
Ge	Cl	39.93	−6.28	46.21
	Br	39.26	−0.69	39.95
	I	36.49	7.96	28.53
Sn	Cl	50.52	−10.73	61.25
	Br	49.47	−4.61	54.08
	I	46.76	4.46	42.30

In keeping with this premonition, Table 6 indicates that none of the TF_3Cl units can form a XB with NH_3. This failure is unsurprising as V_{max} is negative for all of the corresponding systems. For the remaining dimers, the intermolecular distances for the XBs are quite a bit longer than for TB. The XB interaction energies are all quite small, mostly below 2 kcal/mol, as compared to much larger values for the TB, many exceeding 10 kcal/mol. But even so, the reduction in V_{max} for the TBs leaves these interaction energies far smaller than for the TF_3X systems which were more than 30 kcal/mol. As for the perfluorinated systems, the TB interaction energies are only slightly dependent on the nature of the T or X atoms.

Analysis of the wave functions leaves intact most of the conclusions derived from TF_3X. Table 6 shows that the AIM bond critical point densities are much larger for the TBs than for the halogen-bonded systems, as are the NBO second-order perturbation energies for charge transfer from the N lone pair. As for the perfluorinated systems, the exceptions are CH_3X where it is the XB systems that are more strongly bound, along with larger AIM and NBO bond strength measures. And just like the energetics, the replacement of F atoms by H also reduces ρ_{BCP} and $E(2)$ for the tetrel and halogen bonds.

Importantly, whereas most TF_3X molecules were capable of engaging in both a TB and an XB simultaneously, the same cannot be said for TH_3X. It is only for CH_3I that there are trimers identified with the characteristics of containing both TB and XB. This unique ability may be a fortuitous combination of a fairly large V_{max} of 13.9 kcal/mol on I coupled with a long and weak TB that transfers very little charge into the central CH_3I which would otherwise act to dissipate the σ-hole on I. Even so, the halogen bond within this trimer is quite long, with $R(I\cdot\cdot N)$ = 3.225 Å. The halogen bond critical point density is 0.0122 au, and $E(2)$ is equal to 4.21 kcal/mol, both slightly reduced, compared to the XB within the dimer.

■ DISCUSSION

There are a number of interesting aspects of the calculations presented above. One of the chief findings concerns the much greater strength of the TB as compared to the XB. This difference is somewhat surprising in light of their comparable strengths in a very general sense. For example, the interaction energies of the XB in $HBr\cdot\cdot NH_3$ and the TB in $H_4Si\cdot\cdot NH_3$ are equal to 7.8 and 6.8 kcal/mol, respectively.[75] Another study[76] found the TBs of $FH_3T\cdot\cdot NH_3$ were weaker than $FX\cdot\cdot NH_3$ XBs, where T and X were drawn from the same row of the periodic table. These calculations also verified our near equality of the Si and Ge TB interaction energies. The TB and XB in the face of a π-electron donor[77] are roughly equivalent, albeit both are fairly weak. Rough equivalence is also seen between the two sorts of bonds when the electrons arise from an extended π-system.[78] There is some ambiguity, however, in terms of interactions with an anion.[79] When the tetrel bond involves a π-hole on a molecule like XCN, and the XB engages through a σ-hole on X,[80] the latter is more stable than the former, rising up to 8.2 kcal/mol for ICN.

Table 6. Intermolecular N··T/X Distances (Å) between NH_3 and T or X Atoms of TF_3X, Interaction Energies, Bond Critical Point Densities, and NBO Values of $E(2)$ for Transfer from NH_3 N Lone Pair in Complexes of NH_3 with TH_3X

		R, Å		$-E_{int}$, kcal/mol		ρ_{BCP}, 10^{-4} au		$E(2)$, kcal/mol	
		TB	XB	TB	XB	TB	XB	TB	XB
C	Cl	3.125	X	1.93		77		1.74	
	Br	3.208	3.160	1.96	1.32	67	112	1.40	2.66
	I	3.211	3.178	1.69	3.13	69	133	1.43	4.87
Si	Cl	2.483	X	9.18		299		21.18	
	Br	2.403	3.329	10.38	0.65	345	85	25.91	1.04
	I	2.387	3.327	10.60	1.86	357	107	27.99	2.43
Ge	Cl	2.719	X	8.29		210		14.56	
	Br	2.716	3.222	8.30	0.55	212	83	15.45	0.88
	I	2.726	3.341	7.86	1.76	210	104	15.69	2.40
Sn	Cl	2.698	X	12.00		266		15.81	
	Br	2.695	3.451	12.00	0.03	268	70	16.79	0.77
	I	2.711	3.383	11.59	1.27	261	98	17.17	1.94

There have been some comparisons of the TB with pnicogen bonds[31] as well. But what differentiates the data here from prior work is that both the TB and the XB are compared within the context of the same molecule, which contains both a T and X atom. And in this scenario, the TB clearly surpasses the XB in strength, with the sole exception of T = C where this order is reversed.

One of the reasons for the greater strength of the TB as compared to the XB can be laid at the feet of the depths of the σ-holes. V_{max} is considerably larger on the T vs the X atom, by as much as 46 kcal/mol. The ratio of the T σ-hole as compared to X is roughly 2−3. The only exceptions are for T = C where the two holes are comparable or even larger on X as compared to T. And it is for the carbon systems that the XB interaction energy exceeds that of the TB. The attenuation of these σ-holes arising from the replacement of the three F atoms of TF_3X by the less electron-withdrawing H accordingly weakens both sorts of bonds, even to the point of eliminating some of the halogen bonding interactions entirely. But even for these shallower σ-hole Lewis acids, the TB is still far stronger than the XB.

Another distinction between these two bond types rests on the perturbations induced on the Lewis acid. Whereas the internal T−X bond is stretched appreciably when engaged in a TB, the opposite trend of a bond contraction arises when the nucleophile interacts with the X atom. The changes in the ν(TX) stretching frequency are generally consistent with this pattern: large red-shifts for the TBs, with a smaller blue-shift associated with XB formation. The stretches that occur in the covalent bond to the tetrel atom are a common feature of these sorts of bonds,[81−83] especially for the strong TBs with anions.[84] The halogen bond is more diverse in this respect, either stretching[65] or contracting depending on circumstances.

The magnitudes of the tetrel bond energies computed here are consistent with prior work, and many of the trends discussed above for the tetrel bonds to NH_3 are common to other bases such as pyrazine and NCH.[85] For example, as in the data described above, interaction energies of TF_4 with NH_3 were also[81,85] in the 31−35 kcal/mol range and showed little sensitivity to the identity of T for Si, Ge, and Sn. This same sort of insensitivity occurs also when a phenyl substituent is placed on the tetrel atom[86] or when bound to an anion.[84] It was only when monomer deformations were added that the resulting binding energies displayed the expected Si < Ge < Sn trend. These deformations become progressively more important as the substituents on the tetrel atom become bulkier,[82,86] for example, CF_3, isobutyl, or phenyl groups, and are typically of greater magnitude for the smaller T atoms.[84,85] Indeed, large deformation energies are a defining characteristic of tetrel bonds.[87,88]

To place the issue of monomer distortion in the context of the current work, the TB and XB complexes of GeF_3Br are taken as an example. The deformation of this molecule to adopt to the TB dimer requires 18.36 kcal/mol, dwarfing the miniscule 0.08 kcal/mol in the XB complex. The large deformation energy in the TB arises in large part from the "opening of the umbrella" necessary to permit the close approach of the NH_3 unit, which is not an issue for the approach to the halogen atom. Specifically, the θ(BrGeF) angle drops from 111.6° to 98.5°. If these deformation energies are added to the values of E_{int}, then the resulting binding energies of the TB and XB complexes are reduced to 17.2 and 3.4 kcal/mol, respectively. The tetrel bond is still quite a bit stronger than the XB, even if the difference has been diminished a bit.

In a quantitative sense, the bond strengths computed for the bonds presented here are consistent with prior work. Our computed interaction energy for the SnH_3Cl tetrel bond with NH_3 of 12.0 kcal/mol is expectedly higher than an earlier finding[32] of 6.1 kcal/mol for $SnMe_3F$, when one accounts for the electron-donating ability of the three methyl groups that ought to weaken this bond as well as the different level of theory. When paired with a carbonyl donor instead of NH_3, the interaction energies of TH_3F with H_2CO are between 8 and 29 kcal/mol,[89] somewhat larger than the 2−12 kcal/mol range evaluated here for TH_3Cl. This stronger binding is likely due to the greater electronegativity of F vs Cl which would create a much stronger σ-hole on T as well as a different electron donor. The N of a cyano group is an alternate N lone pair donor, albeit a weaker one than NH_3 due to its sp-hybridization. When combined with TH_3F, the interaction energies in the 2−6 kcal/mol range[90] are accordingly somewhat smaller than the TB energies discussed here for $TH_3X + NH_3$ but show the same sort of increase from C to Sn.

One might expect the data to have some sensitivity to the flexibility of the basis set. To test this idea, the tetrel and halogen bond energies of the SiF_3Cl and SiF_3Br units with NH_3 were recomputed with the larger aug-cc-pVTZ basis set, as test cases, incorporating the aug-cc-pVDZ optimized geometries. This enlargement of the basis had only a negligible effect, changing the tetrel interaction energies by only 1 kcal/mol and the halogen bond energies by even less, 0.2 kcal/mol.

A fundamental principle emerging from this work concerns the ability of a tetrel bond to break a pre-existing halogen bond. That is, after a XB complex has been formed, the approach of another nucleophile to the T end of the molecule causes the XB to break entirely and the base to be expelled from the complex. The opposite is not true: each tetrel bond is too strong to be broken by the approach of another nucleophile to the other end of the unit. This finding has important implications for chemical reactivity, catalysis, and macromolecular and crystal structures. It would be worthwhile for future work to consider this same question for other pairs of noncovalent bonds, as to which bonds can simultaneously coexist.

CONCLUSIONS

The TF_3X molecules engage in very strong tetrel bonds with a NH_3 base, with interaction energies on the order of 35−40 kcal/mol. The approach of the base toward the halogen atom is much more tentative, and the XB energies are <6 kcal/mol. (The exceptions are the T = C series where the much weakened TBs place them below the XBs.) Although the T σ-holes grow deeper for larger T and smaller X atoms, there is little corresponding effect of atom size upon the TB interaction energies. While the presence of a halogen bond causes only a minor perturbation upon the strength or length of a tetrel bond, the latter induces a marked stretching and weakening of the former, even causing its disappearance in some cases. Replacement of the three F substituents on TF_3X by H attenuates the σ-holes on both T and X atoms, weakens and stretches both TBs and XBs, and eliminates any halogen bonds involving Cl. Even in those cases where a XB occurs in the dimer, this bond cannot withstand the presence of a simultaneous TB and so disappears.

AUTHOR INFORMATION

Corresponding Author

Steve Scheiner − *Department of Chemistry and Biochemistry, Utah State University, Logan, Utah 84322-0300, United*

States; orcid.org/0000-0003-0793-0369;
Email: steve.scheiner@usu.edu

Complete contact information is available at:
https://pubs.acs.org/10.1021/acs.jpca.0c10060

Notes

The author declares no competing financial interest.

■ ACKNOWLEDGMENTS

This material is based upon work supported by the National Science Foundation under Grant No. 1954310.

■ REFERENCES

(1) Gilli, G.; Gilli, P. *The Nature of the Hydrogen Bond*; Oxford University Press: Oxford, UK, 2009; p 313.

(2) Scheiner, S. *Hydrogen Bonding: A Theoretical Perspective*; Oxford University Press: New York, 1997; p 375.

(3) Jeffrey, G. A.; Saenger, W. *Hydrogen Bonding in Biological Structures.*; Springer-Verlag: Berlin, 1991.

(4) Schuster, P. *Hydrogen Bonds*; Springer-Verlag: Berlin, 1984; Vol. *120*, p 117.

(5) Schuster, P.; Zundel, G.; Sandorfy, C. *The Hydrogen Bond. Recent Developments in Theory and Experiments*; North-Holland Publishing Co.: Amsterdam, 1976.

(6) Gu, Y.; Kar, T.; Scheiner, S. Comparison of the CH···N and CH···O interactions involving substituted alkanes. *J. Mol. Struct.* **2000**, *552*, 17−31.

(7) Alkorta, I.; Sanchez-Sanz, G.; Elguero, J.; Del Bene, J. E. FCl:PCX complexes: Old and new types of halogen bonds. *J. Phys. Chem. A* **2012**, *116*, 2300−2308.

(8) Chalasinski, G.; Cybulski, S. M.; Szczesniak, M. M.; Scheiner, S. Analysis of the potential energy surface of Ar···NH_3. *J. Chem. Phys.* **1989**, *91*, 7809−7817.

(9) Bauzá, A.; Quiñonero, D.; Deyà, P. M.; Frontera, A. Halogen bonding versus chalcogen and pnicogen bonding: a combined Cambridge structural database and theoretical study. *CrystEngComm* **2013**, *15*, 3137−3144.

(10) Alikhani, E.; Fuster, F.; Madebene, B.; Grabowski, S. J. Topological reaction sites - very strong chalcogen bonds. *Phys. Chem. Chem. Phys.* **2014**, *16*, 2430−2442.

(11) Caminati, W.; Evangelisti, L.; Feng, G.; Giuliano, B. M.; Gou, Q.; Melandri, S.; Grabow, J.-U. On the Cl···C halogen bond: a rotational study of CF_3Cl-CO. *Phys. Chem. Chem. Phys.* **2016**, *18*, 17851−17855.

(12) Nziko, V. d. P. N.; Scheiner, S. Chalcogen Bonding between Tetravalent SF_4 and Amines. *J. Phys. Chem. A* **2014**, *118*, 10849−10856.

(13) Del Bene, J. E.; Alkorta, I.; Elguero, J. In *Noncovalent Forces*; Scheiner, S., Ed.; Springer: Dordrecht, Netherlands, 2015; Vol. *19*, pp 191−263.

(14) Szczesniak, M. M.; Chalasinski, G.; Cybulski, S. M.; Scheiner, S. Intermolecular potential of the methane dimer and trimer. *J. Chem. Phys.* **1990**, *93*, 4243−4253.

(15) Mahmudov, K. T.; Gurbanov, A. V.; Aliyeva, V. A.; Resnati, G.; Pombeiro, A. J. L. Pnictogen bonding in coordination chemistry. *Coord. Chem. Rev.* **2020**, *418*, 213381.

(16) Adhikari, U.; Scheiner, S. Comparison of P···D (D = P,N) with other noncovalent bonds in molecular aggregates. *J. Chem. Phys.* **2011**, *135*, 184306.

(17) Metrangolo, P.; Murray, J. S.; Pilati, T.; Politzer, P.; Resnati, G.; Terraneo, G. Fluorine-Centered Halogen Bonding: A Factor in Recognition Phenomena and Reactivity. *Cryst. Growth Des.* **2011**, *11*, 4238−4246.

(18) Latajka, Z.; Scheiner, S. The potential energy surface of $(NH_3)_2$. *J. Chem. Phys.* **1986**, *84*, 341−347.

(19) Politzer, P.; Murray, J. S. In *Noncovalent Forces*; Scheiner, S., Ed.; Springer: Dordrecht, Netherlands, 2015; Vol. *19*, pp 357−389.

(20) Katlenok, E. A.; Haukka, M.; Levin, O. V.; Frontera, A.; Kukushkin, V. Y. Supramolecular Assembly of Metal Complexes by (Aryl)I···d [PtII] Halogen Bonds. *Chem. - Eur. J.* **2020**, *26*, 7692−7701.

(21) Alkorta, I.; Elguero, J.; Frontera, A. Not Only Hydrogen Bonds: Other Noncovalent Interactions. *Crystals* **2020**, *10*, 180.

(22) Grabowski, S. J. Tetrel bond-s-hole bond as a preliminary stage of the S_N2 reaction. *Phys. Chem. Chem. Phys.* **2014**, *16*, 1824−1834.

(23) Bauzá, A.; Mooibroek, T. J.; Frontera, A. Tetrel Bonding Interactions. *Chem. Rec.* **2016**, *16*, 473−487.

(24) Marín-Luna, M.; Alkorta, I.; Elguero, J. A theoretical study of the $H_nF_{4-n}Si$:N-base (n = 1−4) tetrel-bonded complexes. *Theor. Chem. Acc.* **2017**, *136*, 41−48.

(25) Legon, A. C. Tetrel, pnictogen and chalcogen bonds identified in the gas phase before they had names: a systematic look at non-covalent interactions. *Phys. Chem. Chem. Phys.* **2017**, *19*, 14884−14896.

(26) Mani, D.; Arunan, E. The X-C···π (X = F, Cl, Br, CN) Carbon Bond. *J. Phys. Chem. A* **2014**, *118*, 10081−10089.

(27) Varadwaj, P. R.; Varadwaj, A.; Jin, B.-Y. Significant evidence of CO and CC long-range contacts in several heterodimeric complexes of CO with CH_3-X, should one refer to them as carbon and dicarbon bonds! *Phys. Chem. Chem. Phys.* **2014**, *16*, 17238−17252.

(28) Mani, D.; Arunan, E. The X-CY (X = O/F, Y = O/S/F/Cl/Br/N/P) 'carbon bond' and hydrophobic interactions. *Phys. Chem. Chem. Phys.* **2013**, *15*, 14377−14383.

(29) Hou, M.; Zhu, Y.; Li, Q.; Scheiner, S. Tuning the Competition between Hydrogen and Tetrel Bonds by a Magnesium Bond. *ChemPhysChem* **2020**, *21*, 212−219.

(30) Scheiner, S. Comparison of CH···O, SH···O, Chalcogen, and Tetrel Bonds Formed by Neutral and Cationic Sulfur-Containing Compounds. *J. Phys. Chem. A* **2015**, *119*, 9189−9199.

(31) Grabowski, S. J. Pnicogen and tetrel bonds—tetrahedral Lewis acid centres. *Struct. Chem.* **2019**, *30*, 1141−1152.

(32) Franconetti, A.; Frontera, A. Theoretical and Crystallographic Study of Lead(IV) Tetrel Bonding Interactions. *Chem. - Eur. J.* **2019**, *25*, 6007−6013.

(33) Alkorta, I.; Legon, A. An Ab Initio Investigation of the Geometries and Binding Strengths of Tetrel-, Pnictogen-, and Chalcogen-Bonded Complexes of CO_2, N_2O, and CS_2 with Simple Lewis Bases: Some Generalizations. *Molecules* **2018**, *23*, 2250.

(34) Esrafili, M. D.; Asadollahi, S.; Mousavian, P. Anionic tetrel bonds: An ab initio study. *Chem. Phys. Lett.* **2018**, *691*, 394−400.

(35) Liu, M.; Li, Q.; Scheiner, S. Comparison of tetrel bonds in neutral and protonated complexes of pyridineTF_3 and furanTF_3 (T = C, Si, and Ge) with NH_3. *Phys. Chem. Chem. Phys.* **2017**, *19*, 5550−5559.

(36) Hui, Y.-Y.; Bai, C.; Hu, H.-M.; Lv, B.; Wang, X. The effects of the coordination orientation and steric hindrance of ligands on the structural diversity of Pb(II) coordination polymers. *Inorg. Chim. Acta* **2020**, *510*, 119751.

(37) Frontera, A. Noble Gas Bonding Interactions Involving Xenon Oxides and Fluorides. *Molecules* **2020**, *25*, 3419.

(38) Zhu, Z.; Xu, Z.; Zhu, W. Interaction Nature and Computational Methods for Halogen Bonding: A Perspective. *J. Chem. Inf. Model.* **2020**, *60*, 2683−2696.

(39) Berger, G.; Frangville, P.; Meyer, F. Halogen bonding for molecular recognition: new developments in materials and biological sciences. *Chem. Commun.* **2020**, *56*, 4970−4981.

(40) Biot, N.; Bonifazi, D. Chalcogen-bond driven molecular recognition at work. *Coord. Chem. Rev.* **2020**, *413*, 213243.

(41) Yang, H.; Wong, M. W. Application of Halogen Bonding to Organocatalysis: A Theoretical Perspective. *Molecules* **2020**, *25*, 1045.

(42) Saccone, M.; Catalano, L. Halogen Bonding beyond Crystals in Materials Science. *J. Phys. Chem. B* **2019**, *123*, 9281−9290.

(43) Thomas, S. P.; Pavan, M. S.; Guru Row, T. N. Experimental evidence for 'carbon bonding' in the solid state from charge density analysis. *Chem. Commun.* **2014**, *50*, 49−51.

(44) Daolio, A.; Scilabra, P.; Terraneo, G.; Resnati, G. C(sp^3) atoms as tetrel bond donors: A crystallographic survey. *Coord. Chem. Rev.* **2020**, *413*, 213265.

(45) Mooibroek, T. J. Intermolecular Non-Covalent Carbon-Bonding Interactions with Methyl Groups: A CSD, PDB and DFT Study. *Molecules* **2019**, *24*, 3370.

(46) Mundlapati, V. R.; Sahoo, D. K.; Bhaumik, S.; Jena, S.; Chandrakar, A.; Biswal, H. S. Noncovalent Carbon-Bonding Interactions in Proteins. *Angew. Chem., Int. Ed.* **2018**, *57*, 16496−16500.

(47) Trievel, R. C.; Scheiner, S. Crystallographic and Computational Characterization of Methyl Tetrel Bonding in S-Adenosylmethionine-Dependent Methyltransferases. *Molecules* **2018**, *23*, 2965−2981.

(48) Wang, R.; Xiao, B.; Li, W.; Li, Q. Cooperative effects between triel and halogen bonds in complexes of pyridine derivatives: An opposite effect of the nitrogen oxidation on triel and halogen bonds. *Int. J. Quantum Chem.* **2021**, *121*, No. e26429.

(49) Yang, J.; Yu, Q.; Yang, F.-L.; Lu, K.; Yan, C.-X.; Dou, W.; Yang, L.; Zhou, P.-P. Competition and cooperativity of hydrogen-bonding and tetrel-bonding interactions involving triethylene diamine (DABCO), H_2O and CO_2 in air. *New J. Chem.* **2020**, *44*, 2328−2338.

(50) Mó, O.; Montero-Campillo, M. M.; Alkorta, I.; Elguero, J.; Yáñez, M. Ternary Complexes Stabilized by Chalcogen and Alkaline-Earth Bonds: Crucial Role of Cooperativity and Secondary Noncovalent Interactions. *Chem. - Eur. J.* **2019**, *25*, 11688−11695.

(51) Bauzá, A.; Frontera, A. Supramolecular nanotubes based on halogen bonding interactions: cooperativity and interaction with small guests. *Phys. Chem. Chem. Phys.* **2017**, *19*, 12936−12941.

(52) Galmés, B.; Martínez, D.; Infante-Carrió, M. F.; Franconetti, A.; Frontera, A. Theoretical ab Initio Study on Cooperativity Effects between Nitro π-hole and Halogen Bonding Interactions. *ChemPhysChem* **2019**, *20*, 1135−1144.

(53) Esrafili, M. D.; Mousavian, P.; Mohammadian-Sabet, F. The influence of hydrogen- and lithium-bonding on the cooperativity of chalcogen bonds: A comparative ab initio study AU - Esrafili, Mehdi D. *Mol. Phys.* **2019**, *117*, 726−733.

(54) Trujillo, C.; Alkorta, I.; Elguero, J.; Sánchez-Sanz, G. Cooperative Effects in Weak Interactions: Enhancement of Tetrel Bonds by Intramolecular Hydrogen Bonds. *Molecules* **2019**, *24*, 308.

(55) Liu, M.; Li, Q.; Li, W.; Cheng, J. Tetrel bonds between PySiX3 and some nitrogenated bases: Hybridization, substitution, and cooperativity. *J. Mol. Graphics Modell.* **2016**, *65*, 35−42.

(56) Frisch, M. J.; Trucks, G. W.; Schlegel, H. B.; Scuseria, G. E.; Robb, M. A.; Cheeseman, J. R.; Scalmani, G.; Barone, V.; Mennucci, B.; Petersson, G. A.; et al. *Gaussian 09*, Revision B.01; Wallingford, CT, 2009.

(57) Orlova, A. P.; Jasien, P. G. Halogen bonding in self-assembling systems: A comparison of intra- and interchain binding energies. *Comput. Theor. Chem.* **2018**, *1139*, 63−69.

(58) Forni, A.; Pieraccini, S.; Franchini, D.; Sironi, M. Assessment of DFT Functionals for QTAIM Topological Analysis of Halogen Bonds with Benzene. *J. Phys. Chem. A* **2016**, *120*, 9071−9080.

(59) Bauzá, A.; García-Llinás, X.; Frontera, A. Charge-assisted triel bonding interactions in solid state chemistry: A combined computational and crystallographic study. *Chem. Phys. Lett.* **2016**, *666*, 73−78.

(60) Esrafili, M. D.; Vessally, E. A theoretical evidence for cooperative enhancement in aerogen-bonding interactions: Open-chain clusters of $KrOF_2$ and $XeOF_2$. *Chem. Phys. Lett.* **2016**, *662*, 80−85.

(61) Mardirossian, N.; Head-Gordon, M. How Accurate Are the Minnesota Density Functionals for Noncovalent Interactions, Isomerization Energies, Thermochemistry, and Barrier Heights Involving Molecules Composed of Main-Group Elements? *J. Chem. Theory Comput.* **2016**, *12*, 4303−4325.

(62) Forni, A.; Pieraccini, S.; Rendine, S.; Sironi, M. Halogen bonds with benzene: An assessment of DFT functionals. *J. Comput. Chem.* **2014**, *35*, 386−394.

(63) Bauzá, A.; Alkorta, I.; Frontera, A.; Elguero, J. On the Reliability of Pure and Hybrid DFT Methods for the Evaluation of Halogen, Chalcogen, and Pnicogen Bonds Involving Anionic and Neutral Electron Donors. *J. Chem. Theory Comput.* **2013**, *9*, 5201−5210.

(64) Georg, H. C.; Fileti, E. E.; Malaspina, T. Ab initio study of weakly bound halogen complexes: $RX\cdots PH_3$. *J. Mol. Model.* **2013**, *19*, 329−336.

(65) Lu, J.; Scheiner, S. Effects of Halogen, Chalcogen, Pnicogen, and Tetrel Bonds on IR and NMR Spectra. *Molecules* **2019**, *24*, 2822.

(66) Feller, D. The role of databases in support of computational chemistry calculations. *J. Comput. Chem.* **1996**, *17*, 1571−1586.

(67) Schuchardt, K. L.; Didier, B. T.; Elsethagen, T.; Sun, L.; Gurumoorthi, V.; Chase, J.; Li, J.; Windus, T. L. Basis Set Exchange: A Community Database for Computational Sciences. *J. Chem. Inf. Model.* **2007**, *47*, 1045−1052.

(68) Boys, S. F.; Bernardi, F. The calculation of small molecular interactions by the differences of separate total energies. Some procedures with reduced errors. *Mol. Phys.* **1970**, *19*, 553−566.

(69) Brauer, B.; Kesharwani, M. K.; Martin, J. M. L. Some Observations on Counterpoise Corrections for Explicitly Correlated Calculations on Noncovalent Interactions. *J. Chem. Theory Comput.* **2014**, *10*, 3791−3799.

(70) Latajka, Z.; Scheiner, S. Primary and secondary basis set superposition error at the SCF and MP2 levels: $H_3N–Li^+$ and $H_2O–Li^+$. *J. Chem. Phys.* **1987**, *87*, 1194−1204.

(71) Lu, T.; Chen, F. Multiwfn: A multifunctional wavefunction analyzer. *J. Comput. Chem.* **2012**, *33*, 580−592.

(72) Keith, T. A. *AIMALL*; TK Gristmill Software: Overland Park, KS, 2013.

(73) Reed, A. E.; Weinstock, R. B.; Weinhold, F. Natural population analysis. *J. Chem. Phys.* **1985**, *83*, 735−746.

(74) Reed, A. E.; Curtiss, L. A.; Weinhold, F. Intermolecular interactions from a natural bond orbital, donor-acceptor viewpoint. *Chem. Rev.* **1988**, *88*, 899−926.

(75) Dong, W.; Li, Q.; Scheiner, S. Comparative Strengths of Tetrel, Pnicogen, Chalcogen, and Halogen Bonds and Contributing Factors. *Molecules* **2018**, *23*, 1681.

(76) Grabowski, S. J.; Sokalski, W. A. Are Various σ-Hole Bonds Steered by the Same Mechanisms? *ChemPhysChem* **2017**, *18*, 1569−1577.

(77) Ibrahim, M. A. A.; Ahmed, O. A. M.; Moussa, N. A. M.; El-Taher, S.; Moustafa, H. Comparative investigation of interactions of hydrogen, halogen and tetrel bond donors with electron-rich and electron-deficient π-systems. *RSC Adv.* **2019**, *9*, 32811−32820.

(78) Chen, Y.; Yao, L.; Wang, F. Synergistic and antagonistic interplay between tetrel bond and pnicogen bond in complexes involving ring compounds. *J. Mol. Model.* **2019**, *25*, 351.

(79) Del Bene, J. E.; Alkorta, I.; Elguero, J. Anionic complexes of F^- and Cl^- with substituted methanes: Hydrogen, halogen, and tetrel bonds. *Chem. Phys. Lett.* **2016**, *655−656*, 115−119.

(80) Nziko, V. d. P. N.; Scheiner, S. Comparison of p-hole tetrel bonding with s-hole halogen bonds in complexes of XCN (X = F, Cl, Br, I) and NH_3. *Phys. Chem. Chem. Phys.* **2016**, *18*, 3581−3590.

(81) Scheiner, S. Systematic Elucidation of Factors That Influence the Strength of Tetrel Bonds. *J. Phys. Chem. A* **2017**, *121*, 5561−5568.

(82) Scheiner, S. Steric Crowding in Tetrel Bonds. *J. Phys. Chem. A* **2018**, *122*, 2550−2562.

(83) Scheiner, S. The ditetrel bond: noncovalent bond between neutral tetrel atoms. *Phys. Chem. Chem. Phys.* **2020**, *22*, 16606−16614.

(84) Grabarz, A.; Michalczyk, M.; Zierkiewicz, W.; Scheiner, S. Noncovalent Bonds between Tetrel Atoms. *ChemPhysChem* **2020**, *21*, 1934−1944.

(85) Zierkiewicz, W.; Michalczyk, M.; Scheiner, S. Implications of monomer deformation for tetrel and pnicogen bonds. *Phys. Chem. Chem. Phys.* **2018**, *20*, 8832−8841.

(86) Wysokiński, R.; Michalczyk, M.; Zierkiewicz, W.; Scheiner, S. Influence of monomer deformation on the competition between two types of σ-holes in tetrel bonds. *Phys. Chem. Chem. Phys.* **2019**, *21*, 10336−10346.

(87) Lin, H.; Meng, L.; Li, X.; Zeng, Y.; Zhang, X. Comparison of pnicogen and tetrel bonds in complexes containing CX_2 carbenes (X = F, Cl, Br, OH, OMe, NH_2, and NMe_2). *New J. Chem.* **2019**, *43*, 15596−15604.

(88) Solel, E.; Kozuch, S. On the Power of Geometry over Tetrel Bonds. *Molecules* **2018**, *23*, 2742.

(89) Dong, W.; Niu, B.; Liu, S.; Cheng, J.; Liu, S.; Li, Q. Comparison of σ-/π-Hole Tetrel Bonds between TH_3F/F_2TO and H_2CX (X = O, S, Se). *ChemPhysChem* **2019**, *20*, 627−635.

(90) Wei, Y.; Li, Q. Comparison for σ-hole and π-hole tetrel-bonded complexes involving cyanoacetaldehyde. *Mol. Phys.* **2018**, *116*, 222−230.